Preparation and Characterization of Nano-TiO_2 Loaded Bamboo-based Activated Carbon Fibers by H_2O Activation

Dongna Li, Xiaojun Ma,* Xinyan Liu, and Lili Yu

As the support for loading TiO_2, bamboo-based activated carbon fibers (BACFs) were obtained from *Phyllostachys pubescens* Mazel after liquefaction using phenol, melt-spinning, curing carbonization, and H_2O activation. TiO_2/BACFs were prepared by the sol–gel method and characterized by SEM, XRD, FTIR, and XPS. Anatase TiO_2 film with high photocatalytic activity was formed on the surface of BACFs, and the average crystallite size of the TiO_2 film was 17 to 30 nm. The characteristic absorbance peaks of anatase TiO_2 were observed at 1402 and 541 to 605 cm^{-1} on the infrared spectrum of TiO_2/BACFs. The surface of TiO_2/BACFs was mainly comprised of C–C, C–O, C=O, and Ti-O bonds. With increased calcination temperature, the contents of element Ti and Ti-O bonds of lattice oxygen on the surface of TiO_2/BACFs increased and then decreased. The degradation rate of TiO_2/BACFs for methylene blue (MB) solution reached more than 98% after 7 h of UV illumination.

Keywords: Bamboo-based activated carbon fibers; Nano-TiO_2; Loaded; Photocatalyst; Characterization

*Contact information: College of Packaging & Printing Engineering, Tianjin University of Science & Technology, Tianjin 300222, China; *Corresponding author: mxj75@tust.edu.cn*

INTRODUCTION

Nano-TiO_2 has numerous excellent characteristics, including high oxidative property, good stability, low cost, and non-toxicity. However, suspension system powder-type TiO_2 photocatalyst degrades more slowly when the target pollutant content is lower (Vinodgopal *et al.* 1994). Activated carbon fibers (ACFs), with good adsorption and uniform pore structure, have been used as a catalyst support for TiO_2 loading (Uraki *et al.* 2001; Fu *et al.* 2004; Liu *et al.* 2006; Mo and Ye 2009; Yao *et al.* 2010). But ACFs as the support are mainly prepared from fossil resources and are adverse to sustainable use of support materials.

Over the last few decades, some researchers have paid attention to biomass-based activated carbon fibers (Asakura *et al.* 2004; Okabe *et al.* 2005; Senthilkumaar *et al.* 2005; Phan *et al.* 2006; Tan *et al.* 2007; Zhao *et al.* 2010). However, biomass constituents such as cellulose and lignin have been used only to a relatively minor extent. The utilization ratio of raw materials is quite low, which limits the development and application of biomass resources. In recent years, due to the development of biomass liquefaction technique, the liquefaction of biomass materials has been developed for preparing carbon fibers (Ma and Zhao 2010, 2011). This will provide a new method for

the preparation of biomass based activated carbon fibers and biomass photocatalytic composite material.

The objective of this study was to prepare TiO_2-loaded activated carbon fibers from liquefied bamboo powder (TiO_2/BACFs) by the sol–gel method. In order to determine the catalytic performance of TiO_2/ BACFs, the surface structure and characterization of TiO_2/BACFs were addressed in detail. At the same time, the photocatalytic degradation of TiO_2/BACFs for methylene blue (MB) is also discussed.

EXPERIMENTAL

Materials

The raw material was moso bamboo. The powder of 20 to 80 mesh size was dried in an oven at 100 ^oC for 24 h prior to being used. All other chemicals in the study were reagent grade, and they were used without further purification.

Preparation of Photocatalytic Composite Material

A mixture composed of dried bamboo (*Phyllostachys pubescens* Mazel) powder (20 to 80 mesh) and phenol at a mass ratio of 1:6 was liquefied for 2.5 h at 160 ^oC with 8% phosphoric acid (based on the mass ratio of phenol). The as-prepared liquefaction mixture was placed into a reaction tube with 5% hexamethylenetetramine (based on the mass ratio of liquefaction) as the synthetic material. The mixture was heated to prepare the spinning solution, and the initial fibers were prepared by melt-spinning in a spinning machine.

After melt-spinning, the spun filaments were cured by soaking in a solution HCHO and HCl as main components at 95 ^oC for 4 h, washed with deionized water and finally dried. The precursors were activated for 40 min at different activation temperature in a 100 mL/min stream of N_2 and a certain amount of water vapor. BACFs from liquefaction were prepared.

Adding 10 mL of $(TiOC_4H_9)_4$ dropwise into 2/3 ethyl alcohol, solution A was obtained after stirring for 1 h with a magnetic stirring apparatus. Glacial acetic acid was added dropwise into the remaining 1/3 ethyl alcohol, which was mixed with deionized water to obtain solution B. Then, solution B was slowly added to solution A and stirred for 1 h until it became transparent. The mixture was placed in a thermostatic water bath at 35 ^oC for 2 h aging to obtain a milky white colloidal solution. The measured BACFs were put into the solution and vibrated for 30 min. After a certain time of still dipping, the fibers were weighed after drying at 105 ^oC for 2 h, and calcined for several hours in a 100 mL/min stream of N_2, and then naturally cooled. TiO_2/BACFs photocatalytic material was prepared.

Characterization of TiO_2/BACFs

The surface morphologies of TiO_2/BACFs were examined using an SEM (SS-550, SHIMAPZU) device with an acceleration voltage of 15 Kv.

The crystal structures of TiO_2/BACFs were measured with a Power X-ray Diffractometer (D/max-2500, Japan Rigaku) using Cu Kα radiation (wavelength was 0.154 nm, powdery samples), diffraction angle range of 2θ= 5 to 60º with a count time of

20 s at each point. The accelerating voltage and applied current were 40 kV and 100 mA, respectively. The average crystallite size (D) was calculated according to the Scherrer's equation,

$$D = \frac{0.89\lambda}{\beta\cos\theta} \quad (1)$$

where D is the crystallite size (nm), λ is X-ray wavelength (0.154 nm), θ is the Bragg angle of diffraction peaks (°), and β is full width at half maximum (FWHM). The FWHM of each diffraction line was determined from the profile measured with a scanning rate of 1/2° (2θ) min^{-1}, which was calibrated by standard silicon powder for instrumental broadening.

The chemical characterization of functional groups was detected using pressed potassium bromide (KBr) pellets containing 5% of sample by Fourier transform infrared spectrometry (Nicolet-6700, Thermo electron) in the scanning range of 4000 to 400 cm^{-1}.

XPS measurements of the samples at various calcination temperatures were carried out on a Kratos Axis UltraDLD multi-technique X-ray photoelectron spectroscopy with a monochromated Al Kα X-ray source ($h\nu$ = 1486.6 eV). XPS survey spectra were recorded with pass energy of 80 eV and high resolution spectra with a pass energy of 40 eV.

The photocatalytic property of TiO_2/BACFs was determined using a self-made photocatalytic reaction device (darkroom with ultraviolet lamp and magnetic stirring apparatus). A 100 mL sample of methylene blue (MB) solution with a certain content (the maximal absorption wavelength was 665 nm) was used as the target degradation product. Up to 0.1 g of shredded TiO_2/BACFs were poured into the solution to be degraded and stirred for 15 min in a darkroom to reach adsorption equilibrium. Then, the ultraviolet lamp (254 nm) was turned on. After a period of illumination, the absorbance of the sample was measured at 665 nm by ultraviolet-visible spectrophotometry. The degradation rate of MB was calculated using the following equation,

$$\alpha = \frac{A_0 - A}{A_0} \times 100\% \quad (2)$$

where A_0 is the solution content before illumination and A is the solution content after illumination at a moment.

RESULTS AND DISCUSSION

Morphological Characteristics of TiO_2/BACFs

The SEM images of TiO_2/BACFs are shown in Fig. 1. Parts 1 (a), (b), and (c) show that TiO_2 was deposited on almost every BACF with a near-uniform coating thickness. However, cracking and spalling of the formed film were observed on the surface of TiO_2/BACFs. This is due to loose loading of the TiO_2 film before calcination and the shrinkage of TiO_2 film during calcination. Figure 1 (d) shows that some TiO_2 particles were present. It was found that the granular TiO_2 was deposited onto the surface of TiO_2/BACFs during the reaction. Figure 1 (e) shows TiO_2-filled BACFs' pore and not

TiO_2-filled BACFs' pore structure, respectively. This indicates that the pore structure of BACFs is not blocked completely after loading with TiO_2. Such loading evidently did not reduce the absorption performance of the BACFs.

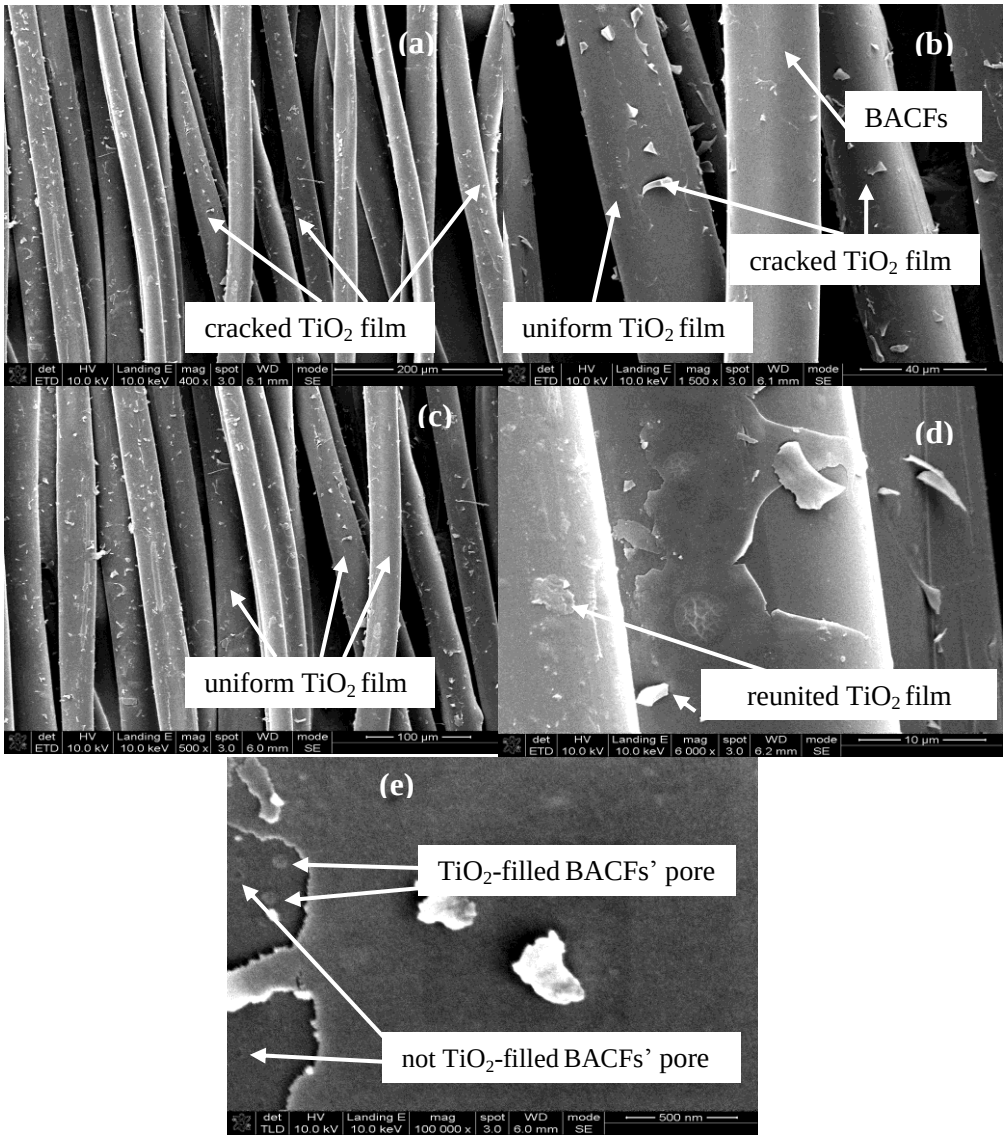

Fig. 1. SEM of TiO_2 loaded on activated carbon fibers（a,b,c,d,e-- Surface）

Effects of Preparation Condition on the Degradation Rate of MB

Figure 2 shows the effect of lighting time on the degradation rate of MB. After 7 h of UV light exposure, the degradation rate of TiO_2/BACFs for MB was 98.12%, 99.06%, 98.76%, and 98.55%, respectively. The product exhibited much higher photo-catalytic activity than commercial TiO_2 (Degussa P-25), about 90% of degradation rate after 7 h of UV illumination (Wang *et al.* 2010, Zhang *et al.* 2013). As the lighting time was extended, the photocatalytic degree of TiO_2/BACFs on MB became enhanced significantly. The best photocatalytic activity was observed at 450 ^oC, and when the temperature was too high or too low, the activity was reduced. This is mainly because

when the calcination temperature was 400 °C, the anatase crystal TiO_2 with high photocatalytic activity was not formed. When the temperature was above 500 °C, particles of nano-TiO_2 would grow and shrink, leading to the enlargement of particle size. As a result, the atoms on the surface decrease quickly and the light adsorption efficiency also decreases, so a saturation state is easily reached, reducing photocatalytic activity (Teruhisa *et al.* 1997).

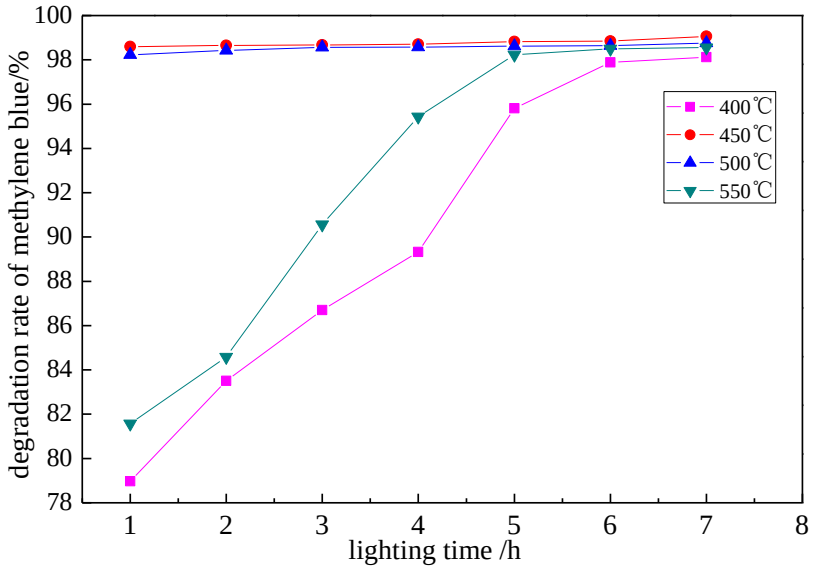

Fig. 2. The effect of lighting time on the degradation rate of MB for samples at different calcination temperatures

XRD analysis of TiO_2/BACFs

Figure 3 shows XRD spectra of TiO_2/BACFs at various calcination temperatures. The diffraction peaks at 25.36°, 37.92°, 48.18°, 53.88°, and 54.94° are attributed to the (101), (004), (200), (105), and (201) planes of anatase TiO_2, respectively. All the TiO_2 films on the surface of BACFs were composed of anatase, indicating that TiO_2 was transformed from an amorphous structure to anatase crystal with high photocatalytic property.

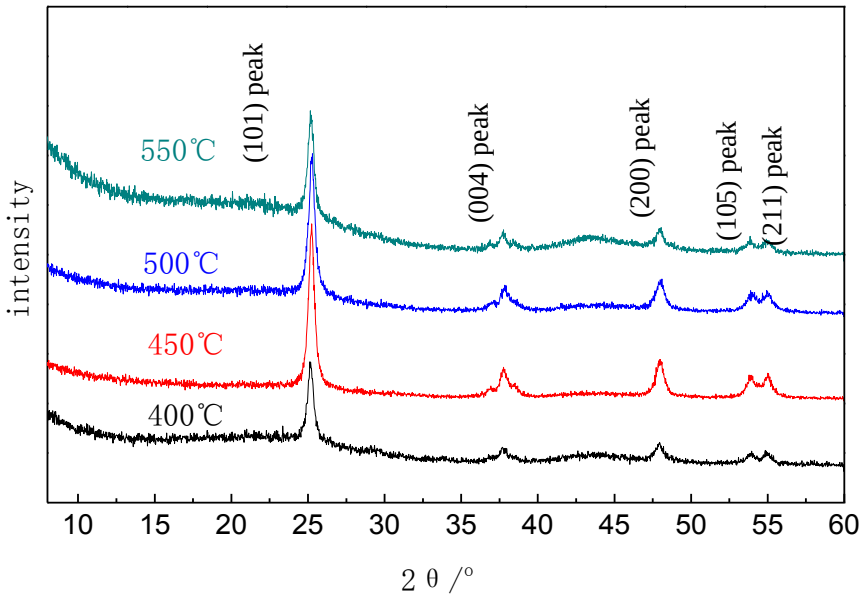

Fig. 3. XRD of TiO_2/BACFs at various temperatures

From Fig. 3, it could be seen that with increased calcination temperature, the diffraction peaks of anatase TiO_2 were narrowed and became more prominent. This means that the crystallization degree of TiO_2 was enhanced. It also has been found that the rutile TiO_2 diffraction peak does not appear (Inagaki *et al.* 2003; Zhang *et al.* 2005; Rong *et al.* 2010), indicating that the high calcination temperature does not lead to the transformation of TiO_2 from anatase to rutile.

Table 1. Relationship between Temperature and Particle Size of TiO_2/BACFs

Calcination temperature/ °C	400	450	500	550
Average crystallite size/ nm	17.09	17.50	25.16	29.11

Table 1 shows the particle size of TiO_2/BACFs as calculated by the Scherrer formula. It could be seen that with increased calcination temperature, the average crystallite size of TiO_2 increased. However, the average crystallite size D was rather small, in the range of 17 to 30 nm and D<< 100 nm, which corresponds to nano-size.

FTIR Analysis of TiO_2/BACFs

Figure 4 shows FTIR spectra of BACFs and TiO_2/BACFs at various temperatures. It could be seen that BACFs and TiO_2/BACFs both presented widely distributed adsorption bands in the range 3200 to 3600 cm^{-1} (-OH). The intensity of the TiO_2/BACFs' stretching vibration (-OH) was slightly larger than that of the BACFs, because the TiO_2/BACFs' vibration was the result of the combined action of phenolic hydroxide (BACFs) and water molecules on the surface of loaded nano-TiO_2. With increased calcination temperature, the adsorption intensity of TiO_2/BACFs gradually decreased. The broad-band adsorption peak began to shift towards higher wave number, with a narrowed peak shape. This indicates that the thermal treatment had removed most of the water from the samples. However, there was still some residual water in the TiO_2. Both BACFs and TiO_2/BACFs showed weak adsorption peaks at 2921 and 2854 cm^{-1}, which were related to C-H. With increased calcination temperature, the strength of two

adsorption peaks increased and then decreased, and the adsorption peaks at 1633 to 1635 cm^{-1} (C=C) also decreased. This suggests that the C=C bond of the samples was not completely damaged during calcination.

BACFs and TiO_2/BACFs present adsorbance peaks near 1402 cm^{-1}. The adsorbance peaks was due to the stretching vibration of aromatic ring C-H. A weak adsorbance peak was also observed in the range 541 to 605 cm^{-1} (Ti-O), which is the characteristic adsorbance range for anatase TiO_2. It indicates that the precursor of Ti was transformed to anatase TiO_2 with high photocatalytic property. As the loading rate of nano-TiO_2 was lowered, its adsorption peak became relatively weak.

In addition, a strong adsorption peak appeared near 1114 cm^{-1}, which corresponds to the P-O-C bond (Rincon *et al.* 2006). The adsorption peak was the result of adding phosphoric acid catalyst during liquefaction.

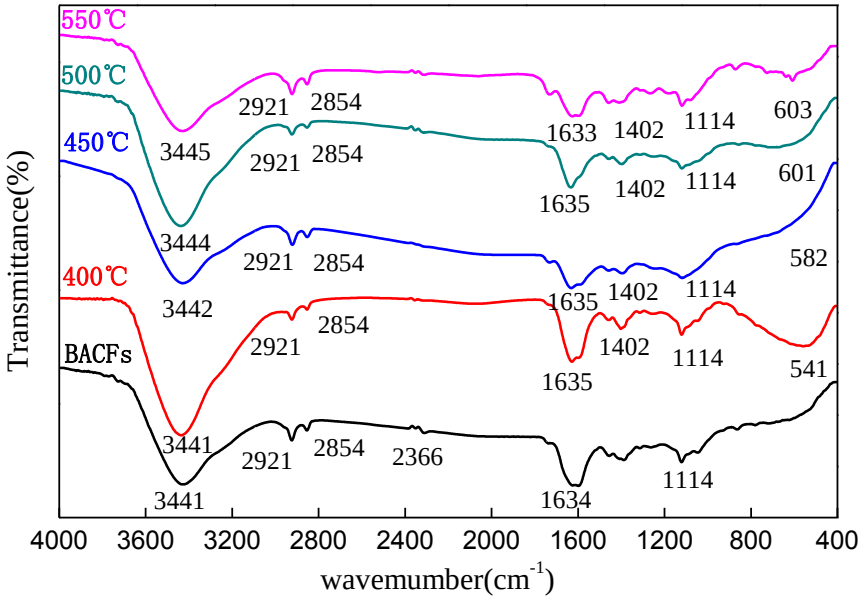

Fig. 4. FTIR of TiO_2/BACFs at various temperatures

XPS Analysis of TiO_2/BACFs

Figure 5 shows XPS spectra of TiO_2/BACFs at various temperatures. These results indicate the presence of primarily C, O, and Ti on the surfaces and relatively smaller amounts of P (Fig. 5(a)). The presence of P could also be explained from the addition of phosphoric acid catalyst for liquefaction. The main elemental composition on the surface of TiO_2/BACFs is shown in Table 2. As seen from Table 2, carbon was found to be the most abundant constituent of all of the samples. With increased calcination temperature, titanium first increased and then decreased. The crystals of nano-TiO_2 became more complete and TiO_2 content increased upon exposure to the proper calcination temperature. However, if the calcination temperature was excessively high, TiO_2 particles would be sintered, and TiO_2 films will contract, crack, and even fall off, which result in fewer elements Ti. By contrast the elements C, O, and P did not exhibit any significant changes in any of the samples.

In order to obtain information about the chemical composition and the binding characteristics of the elements on the surface of TiO_2/BACFs, measurements of the XPS spectra of the C1s, O1s, and Ti 2p region were analyzed. The spectra of four samples

were almost the same; thus only the sample prepared at 450 °C is taken as an example, with its XPS spectra shown in Fig. 5 (b-d). Figure 5(b) indicates that the C1s curve fitting was optimized into three independent peaks: the graphitic carbon (C-C, BE=284.5 eV), ether or hydroxy group (C-O, BE=285.5-285.7 eV), and carbonyl or quinine groups (C=O, BE=286.4-286.6 eV) (Bourgeois *et al.* 1995; Zhang *et al.* 2006; Zhu *et al.* 2011), respectively. It is clear that the loaded nano-TiO_2 did not affect the formation of graphite structure of BACFs.

The XPS spectrum of O1s shown in Fig. 5(c) presents three obvious peaks after peak fitting: the lattice oxygen (O_L), hydroxyl oxygen (O_{OH}), and adsorbed oxygen (O_{ad}), respectively. The former mainly corresponds to Ti-O in the TiO_2 crystal (BE=530.5-530.6 eV). In Fig. 5(d), the binding energy of Ti 2p1/2 and Ti 2p3/2 is 465.0 and 459.3 ev, respectively, with an energy level interval of 5.7 ev. This is consistent with previous studies and indicates that Ti of the TiO_2/BACFs is in the binding state of Ti^{4+} (TiO_2).

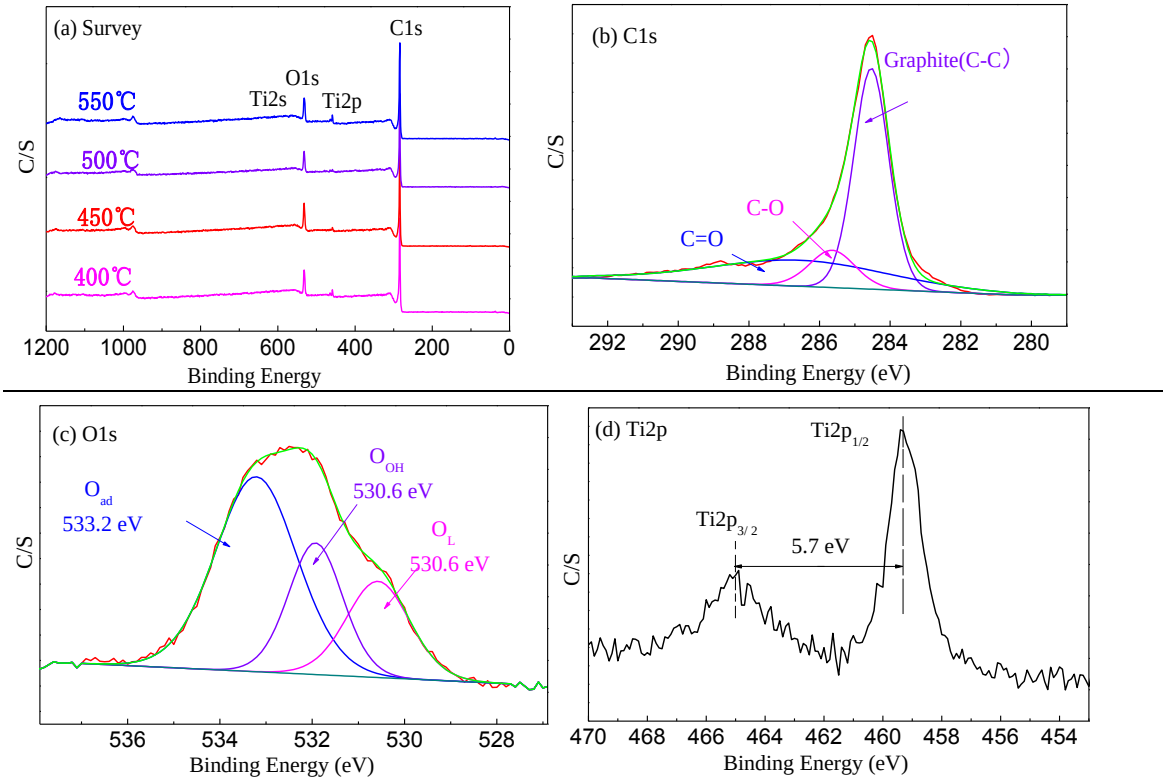

Fig. 5. XPS spectrum of TiO_2/BACFs at various temperatures

Table 2. Elemental Composition of the Surface of TiO_2/BACFs

Calcination temperature (°C)	C1s		O1s		Ti 2p		P 2p	
	BE (eV)	M (%)	BE (eV)	M (%)	BE (eV)	M (%)	BE (eV)	M (%)
400	284.6	80.69	532.3	16.98	459.2	1.80	133.6	0.54
450	284.5	84.62	532.0	9.42	459.1	5.54	133.9	0.42
500	284.5	82.15	532.5	12.39	459.3	5.09	133.7	0.38

550	284.6	80.58	531.9	16.94	459.4	2.13	133.5	0.36

The results of the fits of the C1s and O1s regions are listed in Table 3. It could be seen that the main peak of C1s corresponded to graphitic carbon. With increased calcination temperature, the contents of C-C bond and -OH decreased, while that of C-O and C=O bonds increased overall. Mainly because with the rising of temperature, the graphite carbon involved in the reaction was increased, which broke C-C bonds and formed new C-O or C=O bonds. High-temperature calcination would remove the water molecules contained in the TiO_2/BACFs, resulting in a decrease of -OH. The content of Ti-O bonds first increased and then decreased. This was mainly because the loading degree of TiO_2 on the surface of BACFs was enhanced, with a higher loading rate of TiO_2 and more Ti-O bond. But under higher temperature, the TiO_2 films loaded on the surface of BACFs cracked and finally fell off, so Ti-O bonds showed a lower content.

Table 3. Results of the Fits of the C1s and O1s Regions

T /℃	C-C		C-O		C=O		O_L（Ti-O）		O_{OH}		O_{ad}	
	BE /eV	M /%	BE /eV	M /%	BE /eV	M /%	BE /eV	M /%	BE /eV	M /%	BE /eV	M /%
400	284.5	54.93	285.5	11.37	286.4	33.71	530.5	16.68	531.9	24.48	533.0	58.84
450	284.5	54.15	285.5	12.39	286.5	33.46	530.6	33.06	531.9	17.23	533.2	49.71
500	284.5	53.33	285.7	13.33	286.6	33.34	530.6	25.82	532.0	11.35	533.2	62.83
550	284.5	52.42	285.6	13.29	286.5	34.29	530.6	20.93	531.9	10.56	533.1	68.51

CONCLUSIONS

TiO_2/BACFs were prepared by the sol-gel method and with BACFs as the support, which were obtained after phenol liquefaction, melt spinning, and curing treatment from the phenolated bamboo by H_2O activation. The degradation rate of TiO_2/BACFs on MB improved with longer exposure to UV illumination. All TiO_2 films on the surface of BACFs were composed of anatase with high photocatalytic activity, and the average crystallite size of TiO_2 was 17 to 30 nm. The characteristic adsorption peaks of TiO_2 emerged at 1402 and 541 to 605 cm^{-1} on the infrared spectrum of TiO_2/BACFs. With increased calcination temperature, content of titanium and the amount of Ti-O bonds of lattice oxygen on the surface of TiO_2/BACFs increased and then decreased, with no major changes to C, O, and P contents. Ti was in the binding state of Ti^{4+} (TiO_2) on the TiO_2/BACFs.

ACKNOWLEDGEMENTS

This research was financially supported by National Natural Science Foundation of PR China (No. 30901133, 31270607).

REFERENCES CITED

Asakura, R., Morita, M., Maruyama, K., Hatori, H., and Yamada, Y. (2004). "Preparation of fibrous activated carbons from wood fiber," *J. Mater. Sci.* 39, 201- 206.

Bourgeois, S., Le, S. P., and Perdereau, M. (1995). "Study by XPS of ultra-thin nickel deposits on TiO_2 (100) supports with different stoichiometries," *Surf. Sci.* 328, 105-110.

Fu, P. F., Luan, Y., and Dai, X. G. (2004). "Preparation of TiO_2 photocatalyst anchored on activated carbon fibers and its photodegradation of methylene blue," *China Particuology* 2, 76-80.

Inagaki, M., Hirose, Y., Matsunaga, T., Tsumura, T., and Toyoda, M. (2003). "Carbon coatings of anatase-type TiO_2 through their precipitation in PVA aqueous solution," *Carbon* 4, 2619-2624.

Liu, J. H., Yang, R., and Li, S. M. (2006). "Preparation and application of efficient TiO_2/ACFs photocatalyst," *J. Environ. Sci.* 18, 979-982.

Ma, X. J., and Zhao, G. J. (2010). "Preparation of carbon fibers from liquefied wood," *Wood Sci. Technol.* 44, 3-11.

Ma, X. J., and Zhao, G. J. (2011). "Variations in the microstructure of carbon fibers prepared from liquefied wood during carbonization," *J. Appl. Polym. Sci.* 121, 3525-3530.

Mo, D. Q., and Ye, D. Q. (2009). "Surface study of composite photocatalyst based on plasma modified activated carbon fibers with TiO_2," *Surf. Coat. Tech.* 203, 1154-1160.

Okabe, K., Yao, T., Shiraishi, N., and Oya, A. (2005). "Preparation of thin carbon fibers from waste wood-derived phenolic resin," *J. Mater. Sci.* 40, 3847-3848.

Phan, N. H., Rio, S., Faur, C., Le Coq, L., Le Cloirec, P., and Nguyen, T. H. (2006). "Production of fibrous activated carbons from natural cellulose (jute, coconut) fibers for water treatment applications," *Carbon* 44, 2569-2577.

Rincon, M. E., Trujillo-Camacho, M. E., Cuentas-Gallegos, A. K., and Casillas, N. (2006). "Surface characterization of nanostructured TiO_2 and carbon blacks composites by dye adsorption and photoelectrochemical studies," *Appl Catal B: Environ.* 69, 65-74.

Rong, H. Q., Liu, Z. Y., Wu, Q. L., Pan, D., and Zheng, J. T. (2010). "Formaldehyde removal by Rayon-based activated carbon fibers modified by *P*-aminobenzoic acid," *Cellulose* 17, 205-214.

Senthilkumaar, S., Varadarajab, P. R., Porkodi, K., and Subbhuraam, C. V. (2005). "Adsorption of methylene blue onto jute fiber carbon: kinetics and equilibrium studies," *J. Colloid Interf. Sci.* 284, 78-82.

Tan, I. A. W., Hameed, B. H., and Ahmad, A. L. (2007). "Equilibrium and kinetic studies on basic dye oil palm fiber activated carbon," *Chem. Eng. J.* 127, 111-119.

Teruhisa, O., Dsisuke, H., Kan, F., Kaoru, K., and Michio, M. (1997). "Unique effects of iron(III) on photocatalytic and photoelectrochemical properties of titanium dioxide," *J. Phys. Chem. B* 101, 6415-6419.

Uraki, Y., Nakatani, A., Kubo, S., and Sano, Y. (2001). "Preparation of activated carbon fibers with large specific surface area from softwood acetic acid lignin," *J. Wood Sci.* 47, 465-469.

Vinodgopal, K., Ulick, S., Kimberly, A. G., and Prashant, V. K. (1994). "Eletrochemically assisted photocatalysis. 2. The role of oxygen and reaction intermediates in the degradation of 4-chlorophenol on immobilized TiO_2 particulate films," *J. Phys. Chem.* 98, 6797-6803.

Yao, S. H., Li, J. Y., and Shi, Z. L. (2010). "Immobilization of TiO_2 nanoparticles on activated carbon fiber and its photodegradation performance for organic pollutants," *Particuology* 8, 272-278.

Zhang, S. J., Yu, H. Q., and Feng, H. M. (2006). "PVA-based activated carbon fibers with lotus root-like axially porous structure," *Carbon* 44, 2059-2068.

Zhang, X. W., Zhou, M. H., and Lei, L. C. (2005). "Preparation of photocatalytic TiO_2 coatings of nanosized particles on activated carbon by AP-MOCVD," *Carbon* 43, 1700-1708.

Zhang, D., Xu, B., Zhu, P. J., Lian, Z. H., and Zhao, Y. P. (2013). "Study on the mechanism of methylene blue degradation by TiO_2 photocatalyst," *J. East China Normal Uni. (Natural Sci.)* 5, 35-42.

Zhao, W. X., Bai, Z. P., Ren, A. L., Guo, B., and Wu, C. (2010). "Sunlight photocatalytic activity of CdS modified TiO_2 loaded on activated carbon fibers," *Appl. Surf. Sci.* 256, 3493-3498.

Zhu, N. W., Chen, X., Zhang, T., Wu, P. X., Li, P., and Wu, J. H. (2011). "Improved performance of membrane free single-chamber air-cathode microbial," *Bioresource Technol.* 102, 422-426.

Article submitted: August 21, 2013; Peer review completed: November 6, 2013; Revised version received and accepted: November 19, 2013; Published: December 3, 2013.